On the Exploitation of a High-Throughput SHA-256 FPGA Design for HMAC

HARRIS E. MICHAIL, GEORGE S. ATHANASIOU, VASILIS KELEFOURAS, GEORGE THEODORIDIS, and COSTAS E. GOUTIS, University of Patras, Patras, Greece

High-throughput and area-efficient designs of hash functions and corresponding mechanisms for Message Authentication Codes (MACs) are in high demand due to new security protocols that have arisen and call for security services in every transmitted data packet. For instance, IPv6 incorporates the IPSec protocol for secure data transmission. However, the IPSec's performance bottleneck is the HMAC mechanism which is responsible for authenticating the transmitted data. HMAC's performance bottleneck in its turn is the underlying hash function. In this article a high-throughput and small-size SHA-256 hash function FPGA design and the corresponding HMAC FPGA design is presented. Advanced optimization techniques have been deployed leading to a SHA-256 hashing core which performs more than 30% better, compared to the next better design. This improvement is achieved both in terms of throughput as well as in terms of throughput/area cost factor. It is the first reported SHA-256 hashing core that exceeds 11Gbps (after place and route in Xilinx Virtex 6 board).

Categories and Subject Descriptors: B.7.1 [**Integrated Circuits**]: Types and Design Styles—*Algorithms implemented in hardware, VLSI*; B.6.1 [**Logic Design**]: Design Styles—*Parallel Circuits*

General Terms: Design, Performance, Algorithms

Additional Key Words and Phrases: Hash functions, message authentication codes, fpga, security

ACM Reference Format:
Michail, H. E., Athanasiou, G. S., Kelefouras, V., Theodoridis, G., and Goutis, C. E. 2012. On the exploitation of a high-throughput SHA-256 FPGA design for HMAC. ACM Trans. Reconfig. Technol. Syst. 5, 1, Article 2 (March 2012), 28 pages.
DOI = 10.1145/2133352.2133354 http://doi.acm.org/10.1145/2133352.2133354

1. INTRODUCTION

Hash functions are widely used as sole cryptographic modules or incorporated in hash-based authentication mechanisms like the HMAC, which produce Message Authentication Codes (MACs) [Friedl 2003; NIST-FIPS 2002b]. This kind of security services are used in a many every-day commercial or military applications due to the rapid adoption of e-transactions worldwide varying from transmission of data packets over Internet to authentication services for data storage media. Nowadays, special attention has been drawn on the usage of hash functions/HMAC and other cryptographic algorithms in Internet Security Protocol (IPSec) [NIST:SP800-77 2005] of the forthcoming Internet Protocol (IPv6).

Authors' addresses: H. E. Michail, Department of Electrical Engineering and Information Technology, Cyprus University of Technology, 30 Archbishop Kyprianos St. 3036 Lemesos, Cyprus; email: harris.michail@cut.ac.cy; G. S. Athanasiou, V. Kelefouras, G. Theodoridis, and C. E. Goutis, Department of Electrical and Computer Engineering, University of Patras, 26500 Patra, Greece; email: {gathanas, vkelefour, theodor, goutis}@ece.upatras.gr.

DOI 10.1145/2133352.2133354 http://doi.acm.org/10.1145/2133352.2133354

IPv6 provides several advantages over the current IPv4, and the year 2010 was considered as the beginning of its adoption worldwide [Perset 2008; Pouffary 2000]. Transition to IPv6 is not an option but a necessity as it was also reported by Vint Cerf, the so-called father of Internet [Cerf 2010], since it is going to tackle the address explosion problem allowing to support much more devices than IPv4 [Doraswamy et al. 2003].

In contradiction to IPv4, which was never designed to be secure, IPv6 provides mandatory security services in every transmitted data packet [Pouffary 2000] through the incorporated security protocol IPSec [NIST:SP800-77 2005]. Hence, high-throughput designs for IPSec are necessary in order to handle cryptographic processing of the enormous volume of transmitted data over Internet. Authentication Header (AH) and Encapsulating Security Payload (ESP) are the two main protocols used in IPSec for authentication (AH) and encryption and optional authentication (ESP), respectively.

AH is typically (but not always) built on top of cryptographic hash algorithms such as MD-5 [RFC1321 1992] or SHA-1 [NIST-FIPS 2008]. However, due to security problems that have been discovered in MD-5 [Dobbertin 1996] and SHA-1 [Wang et al. 2005] only the adoption of SHA-2 [NIST-FIPS 2008] in IPSec/IPv6 can be considered as a secure solution. This adoption is expected to happen in the near future. AH uses a Hashed MAC (HMAC) which employs a hash algorithm and a secret value (secret key) to create the HMAC value [NIST-FIPS 2002b]. In the ESP protocol, encryption is provided though the Advanced Encryption Standard (AES) block cipher algorithm, whereas ESP may provide authentication with the same HMAC as in AH [Friedl 2003; RFC4303 2005].

Apart from IPSec, there are many other applications like the Secure Electronic Transactions (SET) [Loeb 1998] and 802.16 standard [Johnston and Walter 2004] for Local and Metropolitan Area Networks that incorporate authentication services. These applications pre-suppose the employment of an authenticating module which includes a hash function. Moreover, digital signature algorithms like DSA [NIST-FIPS 2002a], which are used for authentication services in electronic mail, electronic funds transfer, electronic data interchange etc, are based on using a cryptographic algorithm like hash function. Hashes are also used in Secure Sockets Layer (SSL) [SSL 1998], which is a Web protocol for establishing authenticated and encrypted sessions between Web servers and clients.

All these applications, including IPSec, are used more and more widely lately and often become their host system's bottleneck [Michail 2010]. This drawback becomes severer in case of optical networks that achieve very high-speed transmission rates of over 30Gbits/s. It is clear that there is an urgent need for high-throughput designs of these applications and of IPSec in particular; hence, hardware solutions should be adopted.

There are several published FPGA designs for AES [Hodjat et al. 2004; Granado-Criado et al. 2010] stating very high throughputs (up to 25Gbps). On the other hand, the existing in literature FPGA designs for hash functions and HMAC are below 5Gbps. Since the bottleneck of HMAC performance is the incorporated hash function [Michail 2010], the development of high-throughput designs for the employed hash function is necessary in order to achieve high-throughput security schemes. This will happen since the gap between throughput of hardware designs of HMAC and AES will be significantly reduced. In the case of IPSec this will correspondingly lead to faster data processing and transmission over IPv6.

The rest of the article is organized as follows. Section 2 states the contributions and novelty of the article. Previous work is discussed in Section 3, whereas in Section 4 the background for the HMAC and hash functions is provided. In Section 5 the base architecture for the SHA-256 hash function is presented, and in Section 6 the adopted design methodology is introduced. In the next two sections the proposed architectures

for the SHA-256 hash function and HMAC are presented. The experimental results and comparisons with competitive implementations are provided and discussed in Section 9. Finally, the conclusions are given in Section 10.

2. THE ARTICLE'S CONTRIBUTION

The main contribution of the article is the introduction of a high-throughput and area-efficient design for the SHA-256 hash function. Utilizing Xilinx Virtex-6 FPGA platform the achieved post-place and route throughput exceeds 11 Gbps. In addition, special effort has been paid to keep the occupied area low. It is the first time that such a high throughput is reported for SHA-256 hash function allowing the development of high-performance implementations for security applications where the SHA-256 hash function is the performance's bottleneck (i.e., HMAC in IPSec/IPv6).

The proposed SHA-256 core outperforms the designs proposed by academia or industry in terms of throughput and throughput/area metrics. Implementing the introduced SHA-256 core in the same FPGA technologies with the existing designs, throughput/area and throughput are improved by 30%, compared to the next better performing design. It must be stressed that the increase of throughput has been achieved paying almost no area penalty compared to the next better performing design [Michail et al. 2009].

The improvement of the introduced design has been derived in a systematic way using a proper design methodology. Specifically, the design methodology of Michail et al. [2009], which has been proposed for developing high-performance cores for any hash function, was properly modified and enhanced so as to achieve further optimizations in order to derive improved SHA-256 implementations in terms of throughput and throughput/area cost factors.

Furthermore, it is the first time that implementation details and important modules like the initialization unit for the SHA-256 design are presented. Although initialization unit is necessary to achieve an efficient SHA-256 design when the temporal pre-computation technique is employed, this unit has not been presented in [Michail et al. 2009; Chaves et al. 2008] which exploit this technique to improve throughput. The efficient development of this unit is essential as it allows the use of the temporal pre-computation technique without paying any penalty for extra initialization cycles and without increasing the critical path. Also, special attention has been paid to minimize the area of the introduced initialization unit.

Additionally, extended comparisons between the introduced SHA-256 design and the competitive ones are presented. When the authors first launched optimized SHA-256 design [Michail et al. 2009], only few competitive designs existed, making comparisons somewhat tasteless. However, in the last years a lot of designs for the SHA-256 function have been published. The proposed SHA-256 core is implemented in the same FPGA technologies with the existing designs, leading to extensive and fair comparisons.

Finally, the HMAC and SHA-256 hash function design architectures are presented with information about the internal and handshake signals and synchronization information among different hardware modules.

3. PREVIOUS WORK

A lot of published works on hardware implementations of SHA-256 hash function exist. On the other hand, since HMAC is based on hash functions, there are few works concerning HMAC architecture as a whole, whereas most researchers focus on the incorporated hash function. This is mainly justified since design characteristics of HMAC arise from the corresponding design characteristics of hash functions. However, there are a large number of designs and optimization efforts that have been published for the incorporated hash functions.

Regarding SHA-2 family cores and their optimization towards increased throughput, there is a great research interest the last years. Existing studies can be classified in 3 different classes-generations. The first generation concerns the studies which proposed hardware implementations of hash functions without paying much effort for optimizing these designs in terms of throughput [Ting et al. 2002; Sklavos and Koufopavlou 2005]. Later on, more complex designs and implementations appeared forming the second generation. In these studies [Dominikus 2002; Chaves et al. 2006; McEvoy et al. 2006; Michail et al. 2005] efforts for optimizing frequency and throughput have been made, exploiting techniques like pipeline, resource reuse, and parallelism. The growing need for high-throughput designs for cryptographic schemes led to studies proposing more sophisticated ways to optimize the hardware design of hash functions such as algorithmic optimization techniques (i.e., retiming, precomputation, loop unrolling, etc.) [McEvoy et al. 2006; Glabb et al. 2007; Chaves et al. 2008; Rogawski et al. 2009; Zeghid et al. 2007; Zeghid et al. 2008; Kim et al. 2009; Michail et al. 2009]. These studies form the third generation of the existing works, and almost all of them aim at optimizing the internal transformation round of the corresponding hash functions. The introduced SHA-256 design resides in the third category, as many of the aforementioned algorithmic optimization techniques are exploited.

Although, each of the above-mentioned algorithmic techniques (e.g., retiming, precomputation, loop unrolling etc) offers significant improvements in terms of throughput and throughput/area only in Michail et al. [2009] these techniques were used all together. Hence, compared to all other existing approaches except Michail et al. [2009] the main difference of this study is the utilization of all these algorithmic techniques.

Compared to Michail et al. [2009], the proposed approach has important modifications in the adopted design methodology. Specifically, the methodology presented in Michail et al. [2009] was properly modified for the needs of SHA-256 function by: a) introducing the concept of recursive optimization and b) changing the order of the two last-applied techniques, as it is explained in Section 6, which results in an improved design in terms of throughput and throughput/area metrics.

Beyond academic studies, there are also many commercial SHA-256 Intellectual Property (IP) cores such as CAST's SHA256 IP [CAST Inc.], HELION's SHA256 IP [HELION Technology Ltd], and SoftJin's SHA-256 IP [SoftJin Electronic Design] cores. Although these IPs achieve high throughput and low area, the proposed SHA-256 core outperforms them in terms of throughput and throughput/area ratio.

As long as HMAC as a whole is concerned, Kim et al. [2007] developed a compact and energy efficient HMAC hardware implementation which is capable of supporting the integrity check and command authentication of mobile trusted platforms. The design was evaluated through simulation and synthesis for ASIC implementation and the SHA-1 core is used as hashing algorithm. Khan et al. [2005] developed an HMAC unit employing a unified hash unit that implements the MD5, SHA-1, and RIPEMD-160 hash functions. The authors formed a reconfigurable HMAC module, which implements 6 standard security algorithms and can be reconfigured at runtime to perform any one of them. They also applied the pipelining principle to the proposed HMAC module. The reported throughput was 171.2Mbps, 137.4Mbps and 137.4Mbps using MD5, SHA-1, and RIPEMD-160 hash functions, respectively. In the aforementioned works no detailed information concerning the HMAC architecture and implementation is provided.

4. HMAC AND SHA_256 HASH FUNCTION

4.1. HMAC Function

The purpose of the HMAC is to authenticate the source of a message and its integrity [NIST-FIPS 2002b] by attaching a MAC to the message. MACs are generated

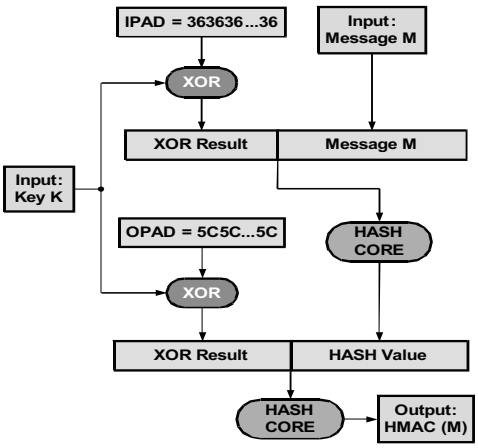

Fig. 1. HMAC algorithmic procedure.

employing two functionally distinct parameters, which are the message input, M, and the secret key, K, whereas the basic component of HMAC is the employed hash function. Specifically HMAC consists of hash and XOR functions. The algorithmic procedure of HMAC is illustrated in Figure 1 [RFC2104 1997].

A hash function breaks up a message into fixed-size blocks and performs an iterative processing over them. For instance, MD5, SHA-1, and SHA-256 hash functions operate on 512-bit blocks, whereas SHA-512 operates on 1024-bit blocks. The size of the output, *HMAC* (M), is the same as that of the underlying hash function (128, 160, 256, or 512 bits in the case of MD5, SHA-1, SHA-256, or SHA-512, respectively), although it can be truncated if it is desired.

The U.S. National Institute of Standards and Technology (NIST) recommends the transition from MD-5 and SHA-1 to the approved SHA-2 family (SHA-224, SHA-256, SHA-384, and SHA-512) of hash functions. At the same time, NIST has also launched a competition for the new SHA-3 hash function standard. Nowadays, this competition is at the Round 3 phase, where the 5 candidates for this round have been chosen and the final winner is expected to be announced in 2012 [NIST-SHA3 2011]. This means that current and future implementations of HMAC utilizing SHA-256 hash function will be used at least until 2020. Hence, the development of high-throughput hardware implementations for SHA-256 hash function and the corresponding HMAC module is important for future applications.

4.2. SHA-256 Hash Function

One way hash functions, $H(M)$, operate on an arbitrary length message, M, and return a fixed-length output, h, which is called hash value or message digest of M. Though there are indefinitely many inputs and only a finite number of outputs, it is computationally infeasible to find two different messages M and M' with the same hash value. For this reason the hash value of M is considered as unique. Given M it is easy to compute h if $H(M)$ is known to both sides. However, given h, it is hard to compute M such that $H(M) = h$, even in cases where $H(M)$ is known. Hash functions are iterative algorithms which in order to compute the hash value perform a number of identical or slightly different operations called *transformation rounds* or *operations*.

According to the employed hash function, the input message, M, of length l is pre-processed (padding). The purpose of padding is to ensure that the input message is a multiple of 512 or 1024 bits (depending on the algorithm). In case of SHA-256, the

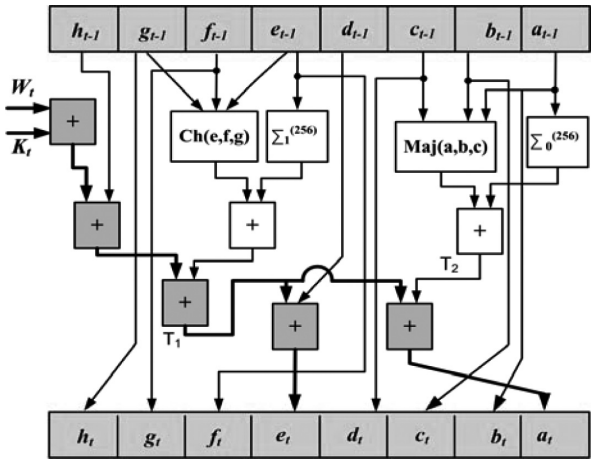

Fig. 2. The SHA-256 transformation round.

message is parsed into blocks of 512-bit and at the end of its last block the bit "1" is appended followed by k zero bits, where k is the smallest, non-negative, solution to the equation $l + 1 + k = 448 \bmod 512$. Then a 64-bit block that is equal to l in binary representation is appended.

The padded data are processed and divided in Message Schedules, W_t, to be used in each transformation round t. Next, the transformation rounds are applied using the message schedules, W_t, the initial hash values,$(H_0^{(0)} - H_7^{(0)})$, and constants, K_t. In case of SHA-256 64 32-bit W_t words are produced by the message scheduling procedure. The hash value is derived by applying 64 transformation rounds (operations). The block diagram of the transformation round is depicted in Figure 2.

The $(a_{t-1} - h_{t-1})$ and $(a_t - h_t)$ boxes represent 32-bit words, whereas W_t and K_t are the message schedules and constants, respectively. It must be noticed that in the first iteration the initial hash values,$(H_0^{(0)} - H_7^{(0)})$, are used as $(a_{t-1} - h_{t-1})$. To produce the output value, each transformation round includes modulo-32 additions and nonlinear functions, which include simple logical functions. The incorporated functions in the transformation round are given in Equation (1).

$$\begin{aligned} Ch\,(x,y,z) &= (x \wedge y) \oplus (\overline{x} \wedge z) \\ Maj\,(x,y,z) &= (x \wedge y) \oplus (x \wedge z) \oplus (y \wedge z) \\ \sum_0^{256}(x) &= ROTR^2(x) \oplus ROTR^{13}(x) \oplus ROTR^{22}(x) \\ \sum_1^{256}(x) &= ROTR^6(x) \oplus ROTR^{11}(x) \oplus ROTR^{25}(x). \end{aligned} \tag{1}$$

The term $ROTR^m$ denotes 'm' times circular right rotation, whereas $\wedge$ and $\oplus$ stand for AND and XOR logical functions, respectively. More details concerning the SHA-256 hash function can be found in NIST-FIPS [2008].

5. SHA-256 CORE—BASE ARCHITECTURE

Concerning the hardware implementation of hash functions the widely used approach for high-throughput designs is the application of four pipeline stages [Michail et al.

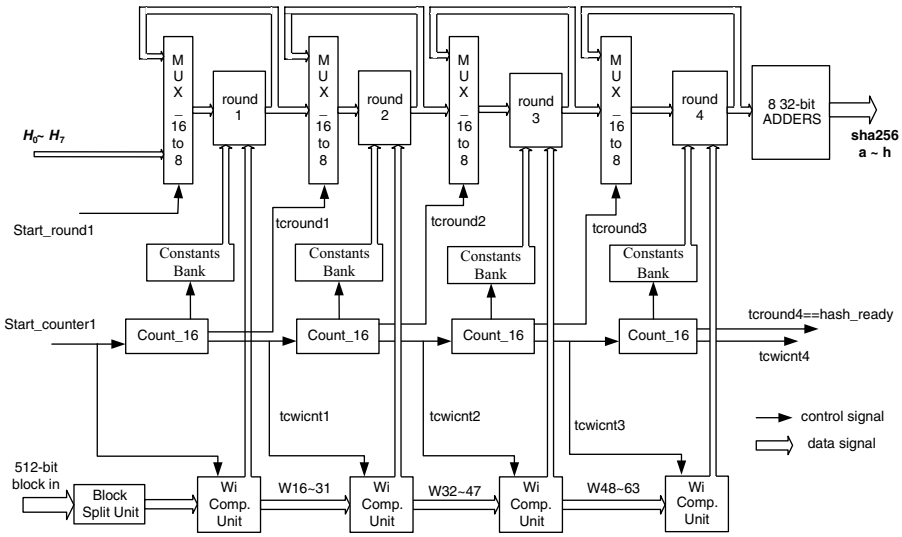

Fig. 3. Base architecture of SHA-256 hash.

2009]. This quadruples throughput by concurrently processing four different messages, while balancing the introduced area penalty with the throughput improvement. The architecture of such design is depicted in Figure 3.

It consists of four pipeline stages called *operational rounds* (round 1, 2, 3, 4 in Figure 3), with a multiplexer in front of each one, while output registers are used at the end of each operational round. Each round corresponds to 16 transformation rounds (operations) of the algorithm, and thus an input message is processed 16 times in each pipeline stage resulting in 64 transformation rounds in total.

The 512-bit input blocks follow the padding formation implemented by a Padding Unit. This unit is implemented in software, since it reduces the complexity of the design without affecting its security level. Also, the constant values, K_t, which are known from the beginning of the transformation, are stored into registers (*Constants Banks*) and serve as inputs in each transformation round.

The 16 to 8 multiplexers are used to input the previous round's outputs (or the initial values for the first round) or to feed back current round's outputs. In combination with the registers they form the 4-stage pipeline ensuring that four different 512-bit data blocks can be processed concurrently and a 256-bit message digest is produced every 16 cycles.

The production of the W_t values is performed by the *Computation Unit* blocks. Each *Wi Computation Unit* consists of: a) one 16 $\times$ 32-bit shift register, b) a 2to1 32-bit multiplexer, and c) a logic module that includes one 4-input adder (32-bit), four 32-bit XOR gates and 6 bit-level rotation blocks, properly arranged for the computation of a W value. This module computes one new W value per clock cycle, whereas its computation time consists of two addition stages, two XOR stages, and one 2 to 1 multiplexer stage, that is $T_{Wi\_Comp\_Unit} = 2t_{XOR} + 2t_{ADD} + t_{MUX}$, where t_{XOR}, t_{ADD}, and t_{MUX} are the delays of the 32-bit XOR, adder, and multiplexer, respectively.

When a 512-bit block is inserted, the first 16 W_t values are produced instantly by performing a simple split in the *Block Split Unit* and fed into the shift register of the first Wi Computation Unit. During the 16 iterations of the first round, the W_{16}-W_{31} values are computed (one per clock cycle) and stored into the unit's shift register through serial input. At the same time, in every clock cycle the appropriate *Wi*

value is fed in the round. When the first round finalizes its computation the computed W_{16}-W_{31} values are transferred (through parallel load) to the shift register of the second W_i Computation Unit. There, the computation of the W_{32} - W_{47} values starts together with the second round's computation. The same procedure takes place for the third and fourth W_i Computation Units, of the third and fourth round, respectively.

The control unit is composed by four *Count_16 Units,* which control all multiplexers. Each *Count_16* component, also arranges the loading of the 16 W_i, in the next round's shift registers. Their outputs are the counting *values* (0_{10} – 15_{10}) and two control signals, *tcwicnt_i* and *tcround_ j,* where *i, j* = 1, 2, 3, 4. The *tcround_4* signal of the 4th *Count_16* unit serves as handshake signal of the whole architecture indicating the computation of the final hash value, whereas the *tcround_ j* (j = 1, 2, 3) signals are used as selectors in the 16 to 8 multiplexers. Each *Count_16* unit is enabled only when there is a message that is being processed in the corresponding transformation round. This way power is saved when no message is supplied for process. When the process in each pipeline stage reaches the end, the *Count_16* component arranges that the process will continue to the next pipeline stage. This is achieved by the control signal *tcwicnt_i*, which serves as enable signal for the *Count_16* unit and selector of the 2 to 1 multiplexor inside the W_i Computation unit of the "$i + 1$" pipeline stage. The enable signal of the first *Count_16* unit and the select signal of the 2 to 1 multiplexor of the first Wi Computation Unit as well, are the core's handshake signal *Start_counter1*. The signal *Start_round1* is the selector of the first 16 to 8 multiplexer. They both indicate the beginning of the hashing process of a new inserted 512-bit input block.

Finally, at the end of the computation, the outputs from the fourth round are fed into 8 32-bit adders to be added with the initial values $a - h$ and produce the final result. This addition consumes less than one clock cycle and does not increase the critical path.

The throughput of a hash function design is equal to:

$$Throughput = \frac{\#bits \times f}{\#cycles}. \tag{2}$$

The term #bits equals to the number of the bits processed by the hash function, the term #cycles corresponds to the required clock cycles to produce a hash value, and f indicates the operating frequency.

Exploring the architecture of Figure 3 and all its components that have been previously analyzed, it is derived that the critical path is located inside the transformation round (between the pipeline stages) and the multiplexer. Thus, to increase throughput, the effort should be focused on the optimization of the operational round.

The operational round of the base SHA-256 function's architecture is illustrated in Figure 2. Taking into account that the nonlinear functions given in Equation (1) are simple logical operations, the delay of each of them is lower than the delay of the 32-bit adder. Therefore, the critical path of base architecture consists of the components that are marked darker in Figure 2. Specifically, it includes four adders for computing a_t or e_t and a multiplexer for selecting the appropriate values for feeding the operational round. Thus, the clock period, T_{base}, of the base architecture equals to:

$$T_{base} = 4t_{ADD} + t_{MUX} \tag{3}$$

6. DESIGN METHODOLOGY

A top-down design methodology for optimizing the throughput for several hash functions including the SHA-256 one has been proposed in Michail et al. [2009]. Specifically, 5 optimization techniques have been proposed and applied leading to a SHA-256 design that achieves 3.3 Gbps throughput in Xilinx Virtex 2 FPGA technology. These techniques exploit specific properties of hash functions, such as the iterative nature

of these algorithms, the use of limited logical and arithmetic operations, and certain spatial and temporal data dependencies.

The methodology that was introduced in Michail et al. [2009] includes the following techniques. The first technique is the *metric partial loop unrolling* where the algorithm is unfolded allowing more operations to be performed in one clock cycle. The best number of operations to be unfolded has been determined by a separate analysis. The second technique is the *spatial precomputation and resources reordering*. At this step, units responsible for the calculation of intermediate values are partitioned appropriately to disjoin in space several dependencies and enhance parallelism. The third technique is the *data prefetching* which precomputes oncecalculated values and feds them in the operational block. Then, at the fourth step *temporal precomputation* of dependant signals is performed. Finally, the fifth technique is the *input compression with Carry Save Adders* (CSAs) units to further reduce the critical path.

However, due to their nonoptimum exploitation in Michail et al. [2009], the last two techniques failed to provide significant improvements compared to the other three ones. In this article a modified and enhanced aspect of this methodology is presented leading to a more efficient way of applying the techniques related to the usage of CSAs and exploitation of temporal precomputation. Also, the concept of recursive application of previously applied techniques (not introduced in Michail et al. [2009]) is included to further improve the critical path and area. This modified methodology results to an optimized SHA-256 design with a reduced critical path compared to Michail et al. [2009].

6.1. Improved Design Methodology for SHA-256 Hash Function

In this work two modifications concerning the optimization process of [Michail et al. 2009] are performed. It is proved that if the optimization process is applied recursively this leads to further improvements to the derived SHA-256 hash function design. Recursive optimization means that after the application of one technique all previously applied techniques are reconsidered for application since in certain cases further improvements can be achieved.

The second modification is related to the order of applied techniques. It has been revealed that if the input compression with CSAs and temporal precomputation techniques are reversed in their order of application, significant performance improvements can be achieved in conjunction with the recursive optimization.

The introduced modified design methodology is illustrated in Figure 4, and in the following paragraphs the aforementioned modifications and their reasoning are discussed.

The algorithmic nature of these techniques leads to a consideration about their recursive application. After the application of each technique, it has to be investigated if some techniques which have already been applied can be reapplied so as to further improve the design. It is clear that additional improvements can be achieved only if an applied technique changes the dependencies between the nodes of the graph (block diagram) of the operational block. In that case a new graph is produced and the re-application of the optimization techniques may offer extra benefits. The recursive process should continue until no improvements are achieved (the graph does not further changes).

The introduced concept of recursive optimization process designates that it is best to apply first those techniques that can benefit the proposed designs not only by their first application but by their reapplication during the recursive process as well. Generally, it is important to apply any technique more than once so as to exploit any opportunity for optimizing the performance of the design.

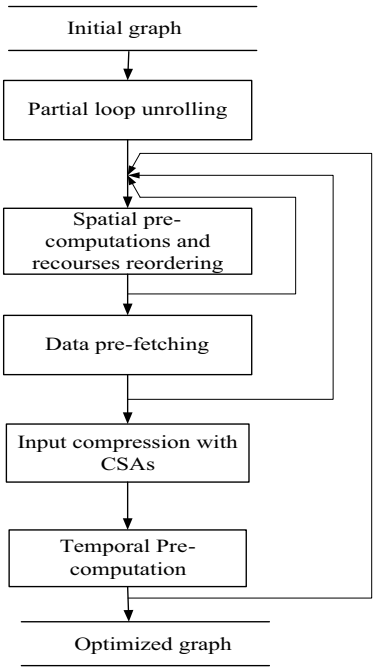

Fig. 4. Improved design methodology.

Due to its nature, the metric partial unrolling is excluded from the recursive process, since it is dependent on the design constraints that are defined before the optimization process begins. Specifically, the unrolling value is determined by a separate analysis based on the area penalty that the designer is willing to pay to improve throughput, whereas the new resulting graph is considered as the feeding graph to the rest optimization process. If the area constraints change, a new analysis will be performed and a new graph will be produced. Hence, the metric partial unrolling technique will be applied first and is excluded from the recursive process.

The spatial precomputations with resources reordering is a changing-graph technique that almost every time leads to significant performance improvements. This technique is quite flexible to be reengineered and offers further optimizations after the application of the rest ones. Moreover, its drastic role in the whole optimization process through the great increase of degrees of freedom and great increase in performance indicates that this technique should be the second one. Also, as it is a changing-graph technique, it will be included in the recursive process.

The third technique targets at data prefetching to the operational block and it is not affected by the internal changes into the operational block, but from the rest system architecture. This is the only technique that its order of appliance is considered neutral, since it is related with the system architecture that is located outside the operational block. Hence, it was decided to be the third technique and, as it is a graph-changing technique, it is included in the recursive process.

Among the last two techniques, the input compression with CSAs is a nonchanging-graph technique as it merges two addition nodes to one with three inputs without moving the nodes or changing the data dependencies of the graph. On the other hand, the temporal precomputation is a changing-graph technique as it moves graph nodes and changes the graph's dependencies, as it will be illustrated in a following section.

Therefore, based on the above reasoning the input compression with CSAs and temporal precomputation should be the fourth and fifth techniques, respectively.

Changing the application order of the last two techniques is based on which of them allows the recursive process to "run" more times, so that these techniques are applied more than once. Specifically, if we choose to apply a nonchanging graph technique (input compression with CSAs) last then the recursive process cannot take place after its application and the optimization stops at this point. On the other hand if a changing-graph technique (temporal precomputation) is applied last then the recursive process takes place allowing all previously applied techniques to be reapplied, leading to further improvements. Indicatively, if the temporal precomputation technique is applied last, after the input compression with CSAs, the recursive process takes place and all the previously applied four techniques are reapplied. During this recursive process, the application of the input compression with CSAs can result in further improvements, since cases of adding three pending values may occur again.

7. PROPOSED SHA-256 DESIGN

In this section, based on the methodology of Section 6, the proposed SHA-256 design is presented in details. For each applied technique, including its recursive application, the produced design is presented and discussed. Also, the achieved operating frequency is given and compared with that of the base architecture.

7.1. Partial Loop Unrolling

First, the algorithm is unfolded using the round unroll technique. In that way, a number of replicas of operations (transformation rounds) are placed together producing a mega-operation block. Placing several operations together allows parallel calculation of independent values resulting in shorter computation times and higher throughput. However, this increases the total area of the design. The best throughput/area ratio for SHA-256 is achieved for two partially unrolled operations. This was determined by a comparative analysis on SHA-256 hash function, based on the derived throughput, the required area, and the calculated throughput/area ratio [Michail et al. 2009].

Partial loop unrolling of two operations means that two consecutive operations are merged resulting in a mega-operation block. This means that the values $(a_{t+1} - h_{t+1})$ are computed based on the $(a_{t-1} - h_{t-1})$ values. This formulation is equivalently expressed by using either t and $t + 2$, or $t - 2$ and t subscripts for input and output values, respectively. The resulted mega-operation block is presented in Figure 5. In the following sections the term *mega-operation* is used to denote two merged operational rounds which are produced by applying the aforementioned loop unrolling.

The critical path of the produced mega-operation block is now longer (6 additions and one nonlinear function are needed to compute the a_t value). Namely, the new clock period, T_1, is given by Equation (4), where t_{nlf} stands for the delay of the nonlinear function:

$$T_1 = 6t_{ADD} + t_{nlf} + t_{MUX}. \tag{4}$$

Compared to Equation (3) the critical path increases by $2t_{ADD} + t_{nlf}$. However, the mega-operation block computes in one clock cycle (T_1) the values that would be computed in two cycles ($2T_{base}$) if the architecture of Figure 2 was used. In addition, since the non-linear function is composed by simple operations, this means that $2t_{ADD} + t_{nlf} < 4t_{ADD}$ thus, $T_1 < 2T_{base}$. Therefore, compared to the base architecture, the unrolled implementation results at a reduction of the total execution cycles form 64 to 32 and hence it improves throughput according to Equation (2).

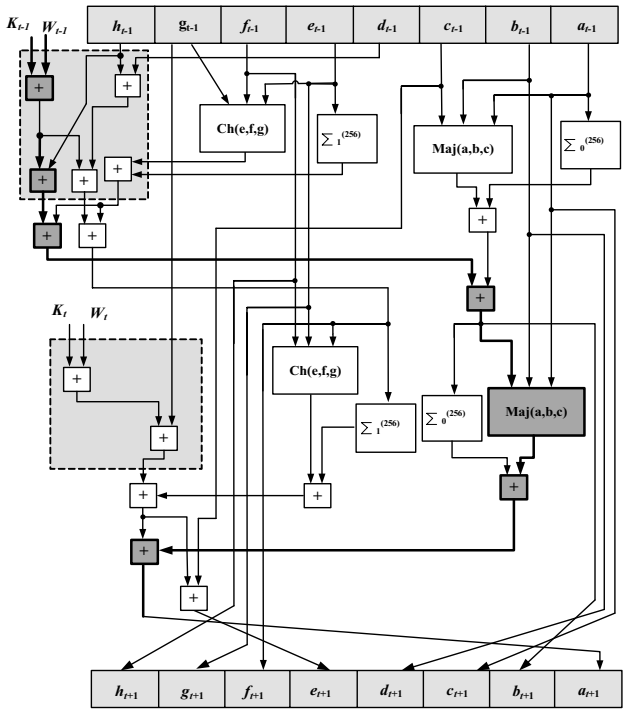

Fig. 5. Two merged SHA-256 operational blocks.

7.2. Spatial Precomputation and Resources Reordering

At this step, certain computational paths which are responsible for the calculation of intermediate values are partitioned appropriately to disjoin several dependencies and allow parallel execution. This is based on the fact that the output values $c_{t+1}, d_{t+1}, g_{t+1}$, and h_{t+1} are derived directly from the input values $a_{t-1}, b_{t-1}, e_{t-1}$, and f_{t-1}, respectively, as shown in Figure 5. Thus, the critical path is determined by the output values a_{t+1}, b_{t+1}, e_{t+1}, and h_{t+1}.

Moving computational resources in mega-operation block, we can spatially precalculate some intermediate values to be used in the next clock cycle. This is applied only to those output values that are derived directly from the inputs. Thus, while the calculations of the current mega-operation are in progress, at the same time some intermediate values that are needed for the next mega-operation can also be in progress of calculation. These precomputations can be mainly achieved by reordering the registers in space. Moving the pipeline stage to a proper intermediate point to store these intermediate calculated values, the critical path is reduced. However, apart from the pipeline registers, any other hardware resource can be moved in order to improve the critical path.

Combining the first two techniques, the operation block is divided into two stages, which are: a) the Precomputation stage, which is responsible for the precomputation of the values which are needed in the next mega-operation, and b) the Postcomputation stage, which is responsible for the final computations of each mega-operation, as shown in Figure 6.

The new critical path, whose components are marked darker in Figure 6, includes four additions, two nonlinear functions (Maj and Ch), and one multiplexer. Thus, the

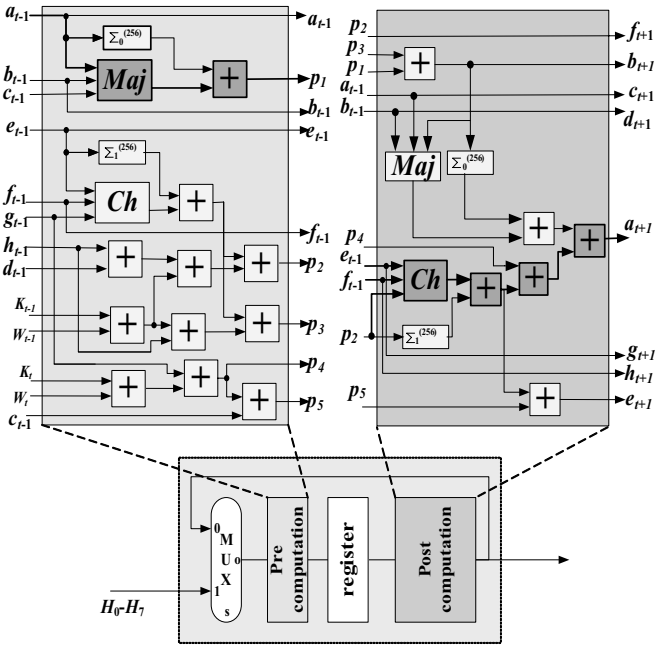

Fig. 6. Operational block after applying the first two techniques.

new clock period, T_2, equals to:

$$T_2 = 4t_{ADD} + 2t_{nlf} + t_{MUX}. \tag{5}$$

Compared to the T_{base}, the new clock period, T_2, is slightly larger due to the two nonlinear functions but it performs in one cycle (T_2) the computations of two operations. On the other hand, the base architecture consumes two clock cycles, ($2T_{base}$) to perform the same computations. Thus, the throughput is improved by 80%–90%.

As the initial graph is reorganized in two subgraphs where the first subgraph corresponds to the Postcomputation stage followed by the Precomputation stage (outputs' feedback via the 16 to 8 Multipexers: Figure 3), it is clear that the spatial pre-computation and resources re-ordering is a changing-graph technique. Therefore, recursive optimization takes place according to the proposed design methodology. However, no extra benefits are achieved through re-application of spatial precomputation and resources reordering and the produced design is that of Figure 6.

7.3. System Level Data Prefetching

The operational block of the SHA-256 function includes the use of constant values K_t and once-calculated values W_t. These values can be precomputed, stored in registers, and fed in the operational block when it is required. Thus, instead of calculating the $W_t + K_t$ values inside the operation block, we can calculate the above sum for a number of W_t and K_t stored values enough time before they are really needed and provide the result directly to the hash core.

Applying this technique to the operation block of Figure 6 does not result in critical path's improvement, because the additions between the constant values are not located in the critical path. However, this technique enables the efficient application and/or reapplication of the other techniques. The derived block after applying the first three techniques is shown in Figure 7.

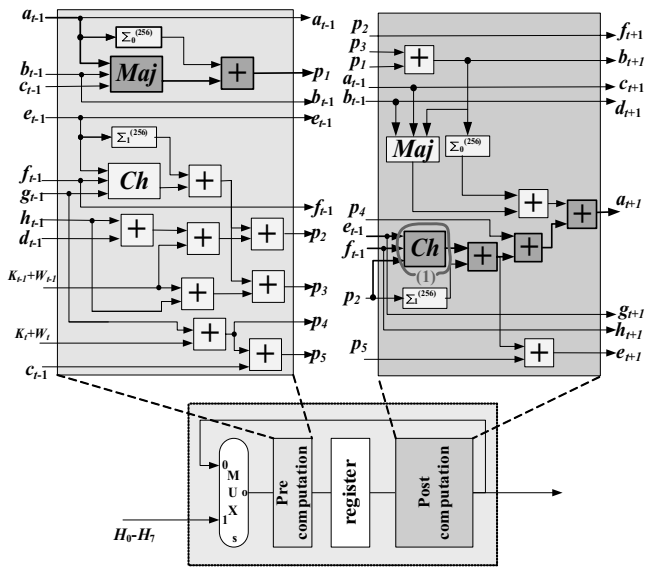

Fig. 7. Operational block after applying data prefetching.

7.4. Recursive Optimization

Based on the modified design methodology the previous applied techniques have to be re-applied. It was explained why metric partial unrolling can not be reapplied, so only the spatial precomputations with resources reordering and the system level data prefetching should be reconsidered.

Investigating Figure 7, it is clear that moving the Ch function (circle 1, in Figure 7) from the Postcomputation to the Precomputation unit improves the critical path because the Ch nonlinear function takes more time to be computed than the function $\Sigma_1{}^{(256)}$. The Ch function can be computed in the Precomputation unit, as the necessary value p_2 is now computed sooner due to the prefetching of values $W_{t+1} + K_{t+1}$ and $W_t + K_t$ to the operational block. The new position of the Ch function is shown in Figure 8 (circle 3) resulting in a new intermediate value p_6. The new critical path, which is marked with darker blocks in Figure 8, consists of: four additions and three non-linear functions. Thus, the new clock period, T_3, equals to:

$$T_3 = 4t_{ADD} + 3t_{nlf} + t_{MUX} \tag{6}$$

Compared to the T_2, the new clock period, T_3, is slightly larger due to the additional nonlinear function. However, the reordering of the "Ch function" enables the efficient application of temporal precomputation technique that will be applied later on and will significantly improve the critical path.

Since the graph's dependencies have been changed as the "Ch function" has moved from the beginning to the end of the graph, the recursive process is reapplied once again. However, reapplying (2^{nd} time) the spatial precomputations with resources reordering no further benefits are achieved and the graph does not change. Hereupon, the reapplication of system level data prefetching is performed leaving the graph unaltered yet again. Thus, the optimization continues with the application of the last two techniques.

7.5. Input Compression with CSAs

The next-applied technique is related to the exploitation of input compressing circuits which in case of SHA-256 hash function these are the CSAs. Due to the nature of

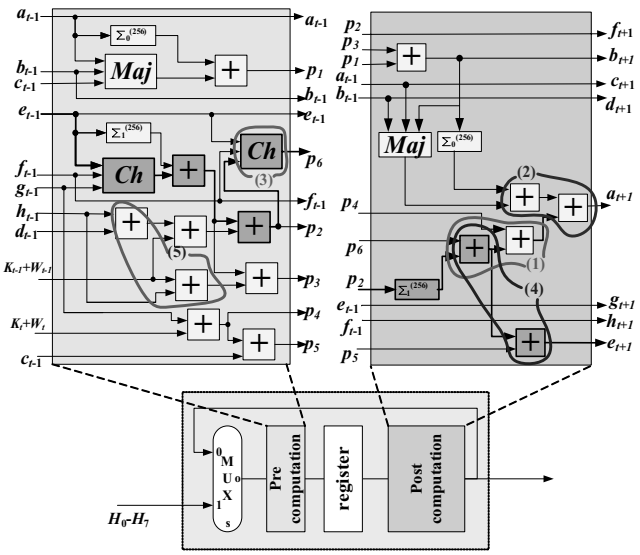

Fig. 8. Reapplication of spatial precomputation and resources reordering.

SHA-256, CSAs can be used as adders which are the main components that contribute to the critical path. Indication for using this technique is the fact that there are some values pending to be added, until a similar process (addition) is ended [Kim et al. 1998].

Specifically, we try to trace cases where it is desired to add more than two pending values together and there is no full exploitation of the delay of the incorporated circuits. For example, adding three values requires the same time as for adding four values. So it is clear that in the case of adding three values there is no full exploitation of the delay of the two addition stages. The addition of the three values could be performed with a CSA resulting in a decreased delay (compared to the two addition stages) and also in an area reduction. In a CSA the delay for adding three values is reduced from two addition stages to one addition stage and the delay of a full adder cell (equal to three logic gates) [Kim et al. 1998].

The critical path of Figure 8 is located on the computation of the value p_6. However, at the beginning of this path while the addition between p_6 and $\Sigma_1{}^{(256)}(p_2)$ is being performed, the value p_4 is pending until the previous addition finishes and thus it can be added in the produced sum (outside of the critical path); this is shown in Figure 8 (circle 1). In that case, the CSA1 is used to add the three values (Figure 9). The same situation occurs for the computation of value a_{t+1} as shown in Figure 8. Thus, the two adders in circle 2 of Figure 8 are replaced by the CSA2 in Figure 9.

Furthermore, since the usage of CSA also results in saving area, cases of merging two adders in one CSA are further investigated. Two such cases are traced. Specifically, the addition of $h_{t-1} + d_{t-1} + (W_{t+1} + K_{t+1})$ in the Precomputation unit (circle 5 in Figure 8) is implemented by the CSA3 in Figure 9. Also, the addition of $p_6 + p_5 + \sum_1^{256}(p_2)$ (circle 4 in Figure 8) is realized by CSA4 (see Figure 9). It has to be stressed that the employed CSA modules consist of a simplistic carry-save tree followed by a modulo-32 addition stage.

Putting together all optimizations we have described, the modified operational block is shown in Figure 9. This block has a new critical path, which is the path for the computation of value p_1 (darker blocks in Figure 9). The new critical path, T_4, equals

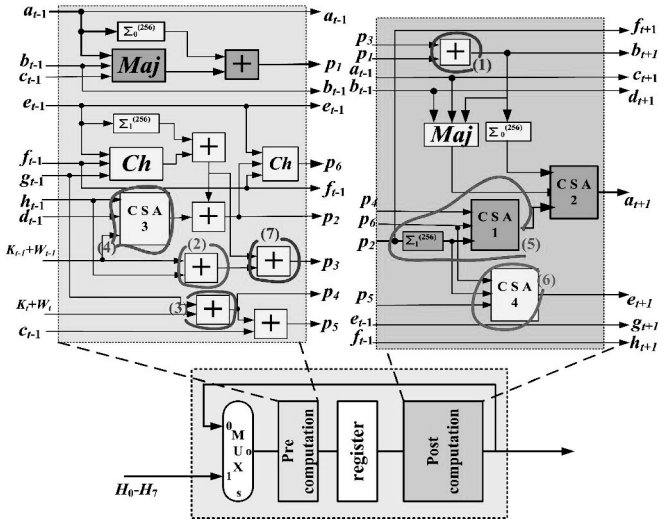

Fig. 9. Input compression exploiting CSAs.

to:

$$T_4 = 2t_{CSA} + t_{ADD} + 2t_{nlf} + t_{MUX}, \tag{7}$$

where, t_{CSA}, t_{ADD}, t_{nlf}, and t_{MUX} are the delays of the CSA, simple adder, nonlinear functions, and multiplexer, respectively.

Since input compression with CSAs is a nonchanging graph technique, the recursive optimization does not take place and the optimization continues with the final technique.

7.6. Temporal Precomputation

Temporal precomputation exploits, by register renaming, the existence of variables which are formed directly from certain inputs, remaining intact in time for a number of transformation rounds before they are consumed. This is of great importance considering that a value may be known for several clock cycles before it is consumed. These variables can be used so as to temporally pre-compute the result of calculations, which typically belong to the critical path and thus reduce it. Usually, these precomputations take place 4 or 5 clock cycles before (as discovered by observing the block of Figure 9).

To make the explanation of temporal precomputation technique compact, let the notation Z_t represent the conjunction of the 8 primary outputs of SHA-256 ($a_t - h_t$) at the t^{th} mega-operation. Then, the mega-operation $t + 1$ is being calculated when the values Z_{t+1} are computed from the values of Z_{t-1}, the values W_t, W_{t+1} and the corresponding K_t, K_{t+1}. Thus, Figure 9 depicts the $t + 1^{th}$ mega-operation.

Inspecting the Postcomputation unit of Figure 9, it can be seen that the current value of p_2 derives directly the value of f_{t+1} at the next mega-operation. Also, the value of f_{t+1} derives directly the value of h_{t+3} at the second following mega-operation. Hence, the value of h_{t+3} is the same as the value of p_2 was two mega-operations earlier. Similar observations also hold for signals e_{t-1} and $d_{t+3.}$ Thus, the following equations are valid:

$$p_2 = f_{t+1} = h_{t+3} \tag{8}$$

$$e_{t+1} = g_{t+3} \tag{9}$$

$$p_1 + p_3 = b_{t+1} = d_{t+3} \tag{10}$$

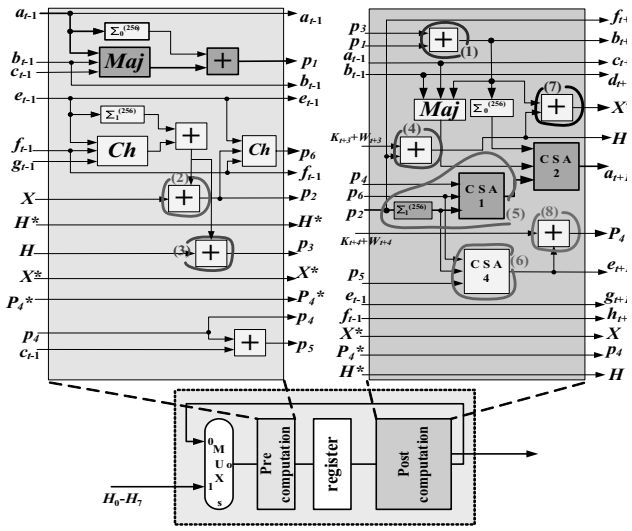

Fig. 10. Operational block after applying the temporal precomputation technique.

Hence, in order to calculate the subsum $W_{t-1} + K_{t-1} + h_{t-1}$, which is used to calculate the value p_3 (circles 2 and 7 in Figure 9), we calculate two mega-operations earlier the subsum $W_{t-1} + K_{t-1} + p_2$ (circle 4 in Figure 10) which is saved into the register H^* at the next mega-operation, as shown in the Postcomputation unit in Figure 10. In the Postcomputation stage of the next operation this value is staying intact by just changing its name into H. Finally, in the Precomputation stage of the second following operation (two clock cycles after the temporal precomputation of the sum) it is consumed with no extra delay (adder in circle 3, Figure 10).

The same also holds for the calculation of values $W_{t-1} + K_{t-1} + h_{t-1} + d_{t-1}$ and $W_t + K_t + g_{t-1}$ (circle 4 and 3 respectively in Figure 9) which are saved in registers X^* and $P4^*$, respectively of the Postcomputation unit, of Figure 10 (circles 7 and 8). Due to the above temporal precomputations, the adders of circles 2, 3, and 4 of Figure 9 are replaced by the adders of circles 4, 8, and 7, respectively in the Postcomputation unit of Figure 10.

Regarding the critical path it remains unchanged. However, temporal precomputation achieves an area reduction by one CSA while the most important fact is that it changes the operational graph. This allows the application of the recursive optimization that will further improve performance, as it will be shown in the next section.

7.7. Recursive Optimization

Since the previously applied technique of temporal precomputation changes the operational graph, recursive optimization takes place according to proposed methodology to further improve performance. For this reason, all previously applied techniques are reconsidered.

First the reapplication of spatial precomputation and resources reordering takes place (3rd reapplication). The adder computing the value $p_3 + p_1$ (in circle 1, Figure 10) is reordered at the end of the Precomputation unit so as to spatially precompute the value $p_3 + p_1$. Moreover, spatial reordering of that part of the critical path, which is responsible for adding $p_6 + p_4 + \Sigma_1{}^{(256)}(p_2)$ and the CSA which adds $p_6 + p_5 + \Sigma_1{}^{(256)}(p_2)$ (circles 5 and 6 in Figure 10, respectively) entirely to the Precomputation unit, is performed, thus improving the critical path as illustrated in Figure 11. Specifically, the

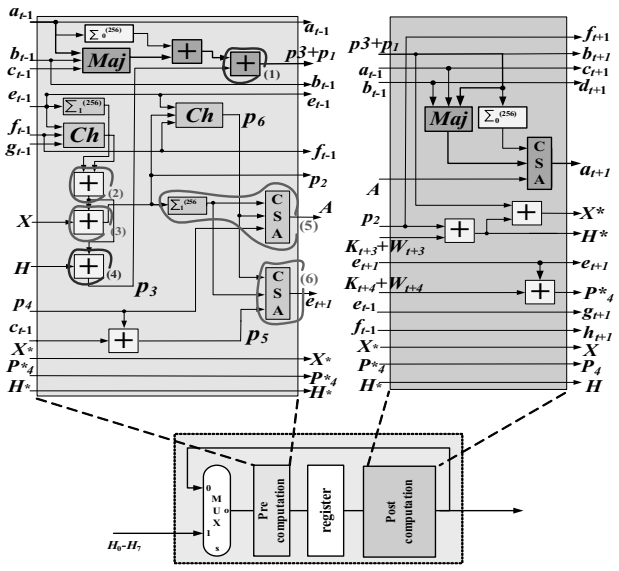

Fig. 11. Operational block after reapplying the spatial precomputation/resources reordering (4^{th} time) and data prefetching (2^{nd} time) techniques.

CSA inside circle 6 bin Figure 10 is the CSA in circle 6 of Figure 11, whereas the CSA and function $\Sigma_1{}^{(256)}(p_2)$ (circle 5, Figure 10) are the CSA and function $\Sigma_1{}^{(256)}(p_2)$ inside circle 5 of Figure 11, respectively. The reordering of the resources of circle 5 of Figure 10 reduces the critical path by $t_{CSA} + t_{nlf}$. In addition, the moving of CSA4 and the resources of circle 1 of Figure 10 leads to balanced paths in the mega-operation block.

Since the graph has changed, by the spatial precomputation and resources reordering technique, the recursive optimization must be applied according to Figure 4. However the reapplication of spatial precomputation and resources reordering technique does not achieve any further improvement. After that we moved on to the reapplication of the third technique related to system data prefetches (2nd reapplication). However, the application of this technique left the graph unaltered without offering further benefit to the design.

Thereafter, we moved on to reapplication of the input compression with exploitation of CSAs technique. In this case, the adder in circle 1 of Figure 11 can be merged with the one computing p_1 resulting in the CSA1 of Figure 12. Furthermore, the adder in circle 2 of Figure 11 can be combined with the one in circle 4 of Figure 11 forming the CSA3 in the Precomputation unit of Figure 12. The adder in circle 2 of Figure 11 can also be combined with the one in circle 3 of Figure 11 forming the CSA2 in the Precomputation unit of Figure 12.

Finally, the reapplication of the temporal precomputation technique takes place. However, the application of this technique left the graph unaltered. Consequently, at this point the optimization process ends and the final operational block of SHA-256 hash function is depicted in Figure 12.

7.8. Final Critical Path

Taking in consideration all changes that have been described it occurs that the critical path has changed and been reduced. New critical path is located in the computation of value $p_3 + p_1$ as highlighted with darker components in Figure 12. Therefore, the final

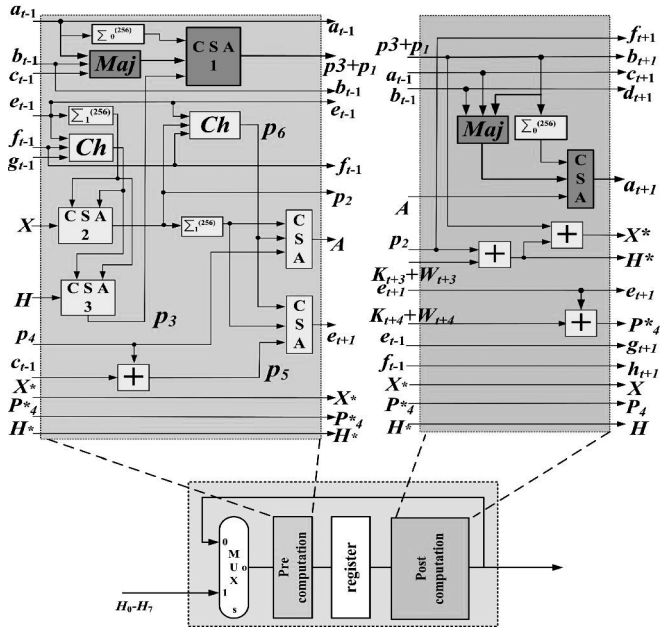

Fig. 12. The final optimized block of SHA-256 hash function.

critical path of the design is given by the following equation:

$$T_5 = 2t_{CSA} + 2t_{nlf} + t_{MUX}. \tag{11}$$

The given critical path is reduced when compared to the one in Michail et al. [2009]. Moreover the integration area penalty was kept low, exploiting the incorporation of more CSAs, resulted by the iterative nature of the improved methodology.

It must be stressed that the above achieved performance improvement comes from the introduced modifications of the design methodology of Michail et al. [2009]. Specifically, the change of application order of the last two techniques along with the recursive optimization leads in the above performance improvement. In contrast, in Michail et al. [2009] where the temporal precomputation was applied before the input compression with CSAs, the application of temporal precomputation did not offer any performance improvement, whereas recursive optimization was not applied. Thus, the proposed design outperforms the design of Michail et al. [2009] in terms of throughput and throughput/area, as it will be shown in the experimental results.

7.9. Proposed Design Architecture of SHA-256 Hash Function

In order to apply the optimization methodology, additional units are needed, the most important of which is the initialization unit. Specifically, to perform spatial and temporal precomputation, certain values must be precomputed and available before the hashing process begins. In particular for the first transformation round, apart from the 8 initial values that are given by the standard ($H_1^0 - H_7^0$), 6 more values have to be computed before the beginning of its first iteration. These values arise taking in consideration the optimization techniques and the resulted transformation round in Figure 12. These values' computation is described by the following equations:

$$X = h_{t-1} + K_t + W_t + d_{t-1} \tag{12}$$

$$H = h_{t-1} + K_t + W_t \tag{13}$$

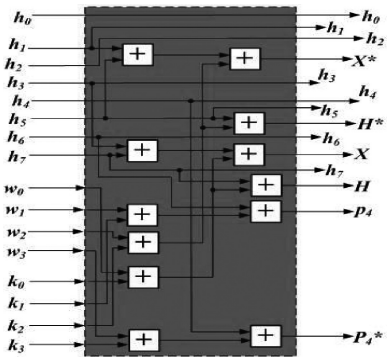

Fig. 13. SHA-256 Initialization Unit.

$$P_4 = K_{t-1} + W_{t-1} + g_{t-1} \tag{14}$$

$$X^* = b_{t-1} + f_{t-1} + K_{t+2} + W_{t+2} \tag{15}$$

$$H^* = f_{t-1} + K_{t+2} + W_{t+2} \tag{16}$$

$$P_4^* = K_{t+1} + W_{t+1} + e_{t-1}. \tag{17}$$

The initialization unit, apart from computing the above values also feeds the first transformation round with the initial values. Its block diagram is illustrated in Figure 13. The above initialization takes place while the system is still receiving the message block (using its first already received part) and ends in less than one clock cycle (in time of 2 32-bit addition stages). Thus, it does not introduce any delay in the proposed SHA-256 hash core. Namely, no extra clock cycles are required and the critical path still resides inside the transformation round.

The detailed architecture of the optimized SHA-256 function, including the Initialization Unit, is presented in Figure 14. Four multiplexers *Mux_26 to 13* in front of each round are employed so as to input the previous round's outputs (or the initial values for the first round) or to feed back current round's outputs. This way a message will be processed for 8 operations in one round and when this process ends in this round, the process will be continued in the next one.

The Block Split Unit is the same as in the base design architecture in Figure 3 whereas the four W_i Computation Units have been slightly modified so as to process and produce 2 W_t in each clock cycle/mega-operation according to the new transformation round in Figure 12. (64 W_t *in total* for the full computation of the message digest). These W_t values are supplied in the "$W + K$" addition block of each round during the process of a message. The four added units, in shadowed blocks in the proposed architecture in Figure 14, compute the '$W_t + K_t$' and '$W_{t+1} + K_{t+1}$' values, which are pre-fetched to the operational rounds. The necessary, K_t and $K_{t+1,}$ constants are stored in the Constants Banks, so as to be added to the appropriate W_t and W_{t+1} respectively, coming from the corresponding W_i Computation Units or the Block Split Unit. The values '$W_t + K_t$' and '$W_{t+1} + K_{t+1}$' are temporarily stored in two 32-bit registers (REG).

Due to the four-stage pipeline, four 512-bit data blocks can be processed at the same time. Each 512-bit input block is processed 8 times in each transformation round resulting in 32 transformations performed in total (in 32 clock cycles respectively). This also means that a 256-bit message digest can be produced every 8 clock cycles. For this reason, the control unit of the whole architecture is composed by four Count_8 Units counting up to 8. The rest functionality and I/O signals of these units are similar to the ones of Count_16 units, illustrated in Figure 3.

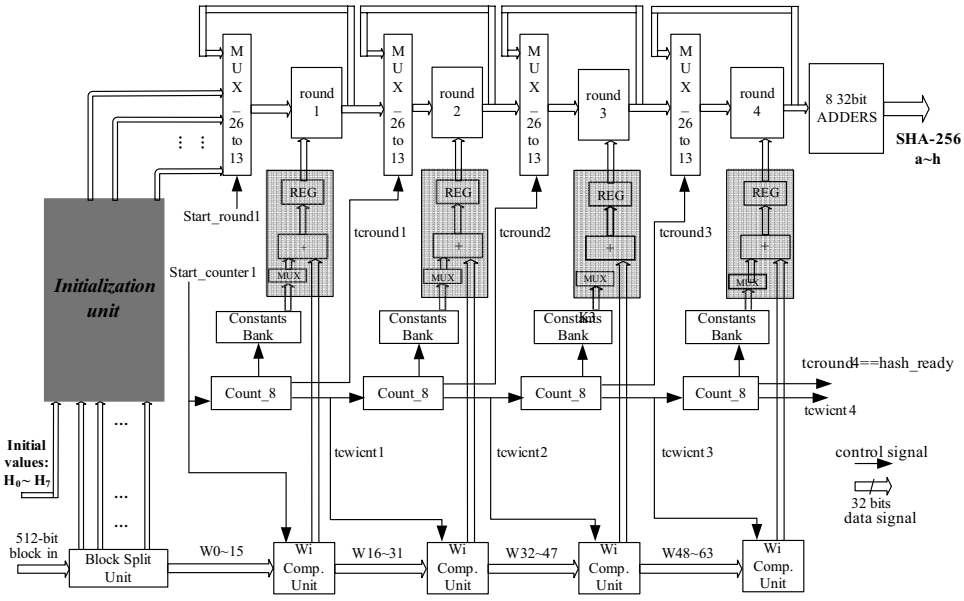

Fig. 14. Final architecture of the SHA-256 hash function.

Finally, when the process of the fourth round ends, its outputs are fed into 8 32-bit adders, where their addition with the initial values ($H_1^0 - H_7^0$) takes place and the final result is produced with no addition of further clock delay. The same handshake signals, as described in base SHA-256 design (Section 5), are used for the communication and synchronization of SHA-256 hash function design with the rest HMAC core.

8. INTRODUCED HMAC DESIGN ARCHITECTURE

HMAC utilizes two hash functions and its output is the same as that of the underlying hash function, (i.e., 256 bits concerning SHA-256). Two SHA-256 hash cores, as designed and presented in the previous section, are used for the proposed HMAC design architecture, which is illustrated in Figure 15.

The HMAC architecture once powers up has to be initialized through activation of the input signal *init*. The initialization procedure corresponds to computing the hash values of two certain 512-bit blocks, which are the corresponding keys, and it is performed independently in the two SHA-256 cores at the same time. The 512-bit Xorskey component contains simple XOR gates to compute the values k0 xor ipad and k0 xor ipad, which are needed in HMAC's initialization. This initialization process is completed after 33 clock cycles.

When the above initialization finishes, the hash values from the outputs of the two SHA-256 cores are stored and then are used as the new initial values ($H_1^0 - H_7^0$) by the two SHA-256 cores. Since these two values and the corresponding keys must be protected and treated as secret, they are stored in registers. This is the first time that a 512-bit message block may be supplied for process to the HMAC core and the *sendmes* handshake signal is activated indicating that the system can accept a new message so as to compute its HMAC value.

Once a message is sent to the HMAC architecture, the handshake signal *new_mes* is activated (for one clock cycle) indicating the arrival of a new input message with input rate of 64 (or more) bits per clock cycle depending on the employed bus width. At the same time *sendmes* signal is deactivated (and stays deactivated) and the system

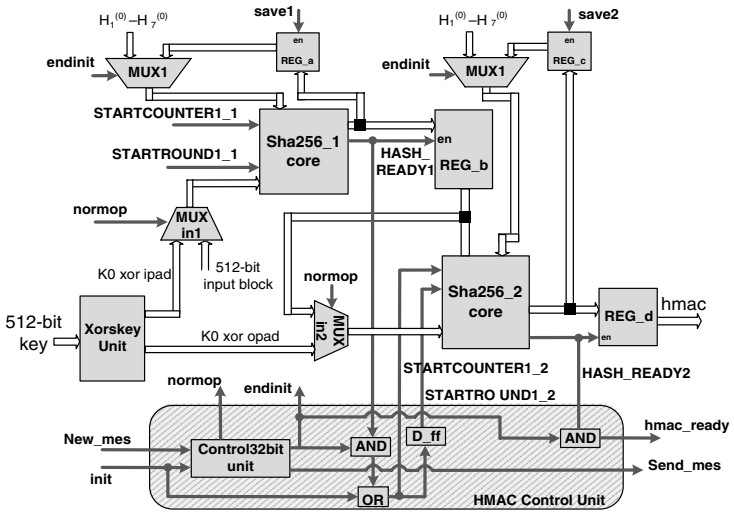

Fig. 15. Proposed HMAC-SHA-256 architecture.

starts formulating the 512-bit input message block which is over after 8 (or less) clock cycles (depending on the selected bus width). During these cycles, (and while another message may be in process on any stage of the two SHA-256 hashing cores) the first 128 bits of the 512-bit input message block are used to perform the necessary initializations in the Initialization Unit, (Figure 14) of the first SHA-256 hashing core. This initialization ends in one clock cycle (Section 7.9). After these 8 clock cycles have pass the processing on the first transformation round of the first SHA-256 hash core begins and the *sendmes* signal is activated again indicating that a new input message can be supplied to the HMAC design.

The message that entered in the first SHA-256 core is processed, and finally after 32 clock cycles its 256-bit hash value exits the first SHA-256 core. It is then stored in the intermediate register *REG_b*, along with padding bits and length information about the input message block in the second SHA-256 hashing core (message length is always the 256 bits that are produced from the first SHA-256 hashing core).

The 256-bit hash value beyond the register *REG_b*, also feeds the initialization unit of the second SHA-256 core. So in the clock cycle that is needed for formulating the 512-bit input message for the second SHA-256 core (from the 256-bit output hash value from the first SHA-256 core), also the initialization for processing this message at the second SHA-256 core has been performed (at corresponding unit of the second SHA-256). Moreover in the same clock cycle the necessary signals are generated so as to enable process at the second SHA-256 hashing core at the very next clock cycle.

Then the rest process for the HMAC value computation begins in the second SHA-256 hashing core which is also finalized after 32 clock cycles. Finally after 65 clock cycles in total (32 for each one of the two SHA-256 cores and one clock cycle for the intermediate *REG_b* padding-register), the final HMAC value is computed. One clock earlier the handshake signal *Hmac_ready* is activated so as to notify the host system that at the next clock cycle the HMAC value can be retrieved.

In the presented HMAC core, every 8 clock cycle a new message can be inserted for computation of its HMAC value. The utilized SHA-256 hashing cores incorporate four pipeline stages each. Thus, taking into consideration that the message receiving phase which lasts 8 or less clock cycles, it occurs that 9 different messages can be concurrently processed.

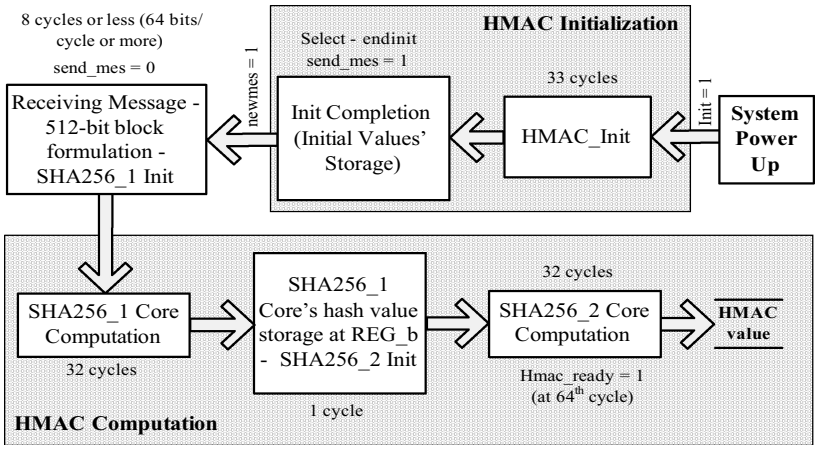

Fig. 16. HMAC computation flow.

In normal operation, inputs ($H_1^0 - H_7^0$) are the hash values that were computed during the initialization process and are now treated as the new keys. When a new key should be used then the signal *init* is activated and a new HMAC initialization phase is taking place. The described HMAC computation procedure is presented in the computation flow shown in Figure 16.

Finally, the Control Unit produces the control signals used inside the HMAC core as well as the handshake signals (the functionality of which was described previously) which are used for communication and appropriate synchronization with the rest platform.

9. EXPERIMENTAL RESULTS AND COMPARISONS

The introduced architectures of the SHA-256 hash function and HMAC mechanism were captured in VHDL. Their correct functionality was verified through Post-Place and Route (Post-P&R) Simulation via the Model Technology's ModelSim Simulator. A large set of test vectors, apart from the test example proposed by the standard, were used. Beyond that, downloading to actual FPGA boards was performed and the implementations' correct functionality was verified via ChipScope. Many FPGA technologies were selected to implement the proposed designs such as FPGA families Virtex, Virtex II, Virtex II Pro, Virtex E, and Virtex 4. The above FPGA families were chosen for comparison reasons since a lot of SHA-256 designs have been synthesized on them and reported in the literature. Moreover, experimental results after place and route (P&R) were taken for FPGA families Virtex 5 and Virtex 6. The tool used for synthesis, mapping, and P&R the introduced designs to the targeted technologies was the XST synthesis tool of Xilinx ISE Design Suite.

It has to be mentioned that there is a limited amount of HMAC designs in FPGA published by academia or industry. This is because the relevant research is focused on the optimization of the main module of the HMAC mechanism which is the utilized hash function. It is obvious from the HMAC architecture that the operating frequency and throughput of HMAC mechanism is determined by the SHA-256 hash function module. Hence, in order to make a fair comparison, we choose to provide separately

References	Freq. (MHz)	Throughput (Mbps)		Area (slices)
		Synthesis	P&R	
[Dominikus 2002]	42.9	77	-	2008
[Ting et al. 2002]	88	87	-	1261
[Sklavos et al. 2005]	83	326	-	2120
[Chaves et al. 2006]	82	646	-	764
[Glabb et al. 2007]	77	308	-	1306
[Chaves et al. 2008]	82	646	-	764
[Rogawski 2009]	-	856	-	
[Michail et al. 2009]	46.8	2995	-	3192
Proposed	**58,7**	**3757**	**3667**	**2943**

(a)

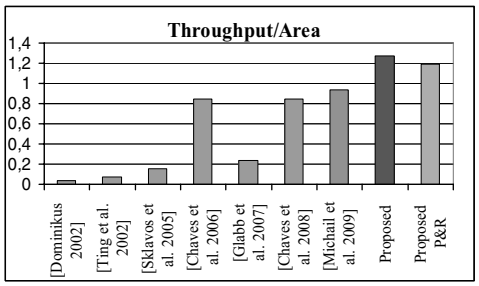

(b)

Fig. 17. SHA-256 – Xilinx Virtex family results.

References	Freq. (MHz)	Throughput (Mbps)		Area (slices)
		Synthesis	P&R	
[Chaves et al. 2006]	150	1184		797
[McEvoy et al. 2006]	133	1009		1373
[Chaves et al. 2008]	150	1184		797
[Zeghid et al. 2007]	81	1296		1938
[Zeghid et al. 2008]	56	896		1480
[Kim et al. 2009]	71.5	74,7		779
[Rogawski 2009]		1992		
[CAST Inc.]	120		930	815
[Michail et al. 2009]	70.1	4485		2862
Proposed (-6)	**98.9**	**6330**	**4768**	**3075**
Proposed (-5)	**85,9**	**5498**	**4132**	**3077**

(a)

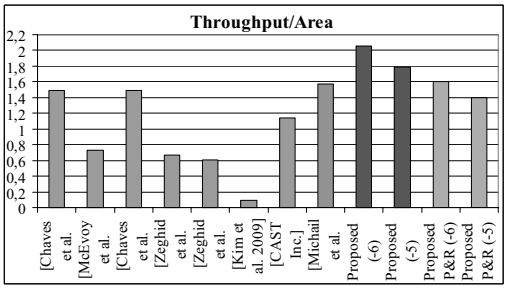

(b)

Fig. 18. SHA-256 – Xilinx Virtex II family results.

detailed comparisons for the SHA-256 hash function, for which there exist many implementations proposed either by academia or industry. However, the implementation results of the proposed HMAC architecture are also provided.

In addition to frequency, throughput, and the occupied area, the fairer comparison and evaluation factor which is throughput/area ratio is also included. As different optimization techniques were applied on each design including the proposed one and these presented in the literature, it results in designs and implementations with different throughput and area values. Hence, to fairly evaluate the quality of each implementation, the throughput/area ratio is adopted in our study.

It must be stressed that in order to have a fair comparison, the architecture of Michail et al. [2009] was remapped using the Xilinx ISE Design Suite since a different synthesis tool was employed in Michail et al. [2009]. This proves that the achieved improvement is due to the modified optimization procedure that was proposed in this paper and the resulted optimized SHA-256 hash core and not due to the usage of more sophisticated and modern synthesis tools.

In Figures 17–21 the implementation results and comparisons between the proposed and existing SHA-256 hash designs are presented. Each figure includes a table where the area, frequency, and throughput values are provided and a chart where the corresponding throughput/area ratios are illustrated.

Concerning the throughput of the introduced architectures, two different values are provided, namely the value that is arisen after synthesis (post-synthesis) and that is derived after place and route (P&R). Also, as the area, frequency, and throughput strongly depend on the speed grade, we also provide the speed grade values that were used to implement the proposed architectures.

References	Freq. (MHz)	Throughput (Mbps)		Area (slices)
		Synthesis	P&R	
[Chaves et al. 2006]	174	1370		755
[Chaves et al. 2008]	174	1370		755
Proposed (-7)	**118.1**	**7558**	**6375**	**3054**

(a)

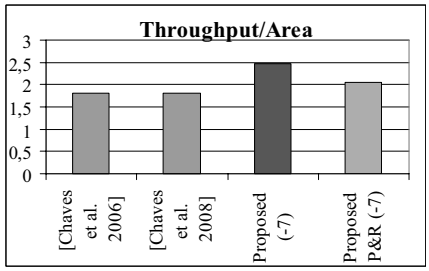

(b)

Fig. 19. SHA-256 – Xilinx Virtex II Pro family results.

References	Freq. (MHz)	Throughput (Mbps)		Area (slices)
		Synthesis	P&R	
[Michail et al. 2005]	64.1	2052		2930
[Michail et al. 2009]	49.1	3142		3006
Proposed (-8)	**66.8**	**4275**	**3968**	**3181**
Proposed (-6)	**52.5**	**3360**	**3187**	**3190**

(a)

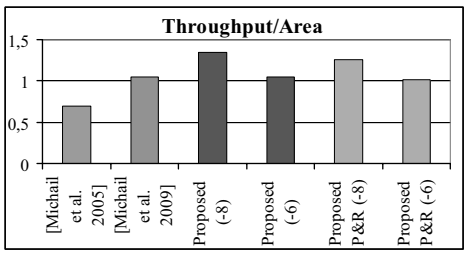

(b)

Fig. 20. SHA-256 – Xilinx Virtex E family results.

References	Freq. (MHz)	Throughput (Mbps)	Area (slices)
[CAST Inc.]	144	1116	829
[HELION Tech. Ltd]	162	1256	758
[SoftJin Electronic Design]	139	1079	754
Proposed P&R	**130,1**	8326	**3963**

(a)

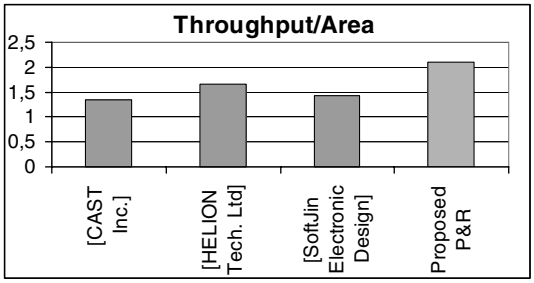

(b)

Fig. 21. SHA-256 – Xilinx Virtex 4 family results.

Regarding the Xilinx Virtex family (Figure 17), the proposed SHA-256 hash function architecture achieves an operation frequency equal to 58.7 MHz, whereas the throughput after synthesis equals to 3.8 Gbps and 2,943 slices were devoted for its implementation. Also, the throughput/area ratio equals to 1.02. Compared to the existing designs implemented on this technology, the proposed one outperforms them in terms of throughput (26% up to 4,780%) and throughput/area ratio (33.6% up to 3.229%).

The proposed design was implemented in Virtex II FPGA family (Figure 18) with speed grade values 6 and 5. Compared to the competitive implementations, the proposed one (with speed grade equal to 6) outperforms them both in throughput (40.3% up to 8,373.9%) and throughput/area ratio (30.6% up to 2,046%). Also, compared to the design of CAST Inc, using the post place route values the throughput improves by 412%.

Table I. Implementation Results of the Proposed SHA-256 Hash Design in Xilinx Virtex 5 and Virtex 6

Platform	Freq. (MHz)	Throughput (Mbps)	Area (Slices)
Virtex $5^{(-3)}$	169	10816	1885
Virtex $6^{(-3)}$	172	11008	1831

Table II. Implementation Results of the Proposed HMAC Architecture

Platform	Freq. (MHz)	Throughput (Mbps)	Area (Slices)
Virtex	50.1	3,206	6,964
Virtex II (−5)	65	4,130	6,832
Virtex II (−6)	70.6	4,521	6,835
Virtex II RRO (−7)	96.3	6,163	6,789
Virtex E (−6)	49.5	3,168	6,874
Virtex E (−8)	60.2	3,852	6,883
Virtex 4(−12)	130.1	8,326	7,123
Virtex 5(−3)	163.8	10,483	4,219
Virtex 6(−3)	170.1	10,886	4,028

Also, in Virtex II PRO and Virtex E families (Figures 19 and 20, respectively) the introduced architecture achieves higher throughput and throughput/area values. Specifically, in Virtex II PRO the throughput and throughput/area ratio are improved by 451.7% and 36.4%, respectively, whereas the corresponding improvements in Virtex E technology are 36.1% and 28.6%, respectively.

Additionally, the proposed SHA-256 architecture is compared to commercial SHA-256 implementations in Virtex 4 technology (Figure 21). In this case only the post place and route values (P&R) are used for comparisons.

Again the proposed implementation outperforms the competitive ones both in throughput (562.9% up to 671.6%) and throughput/area ratio (70.2% up to 109.4%). Apart from the above reported results, the proposed SHA-256 design was also implemented in Xilinx Virtex 5 and Virtex 6 FPGAs. The implementation results (Post P&R) are presented in Table I.

As is shown in Table I, the achieved throughput after place and route in Virtex 6 technology exceeds 11 Gbps.

Furthermore, the introduced SHA-256 hash core was compared with a conventional 4-stage pipeline (see Figure 3) where no special optimization effort has been paid to optimize the operation block. This was done so as to exhibit the efficiency of the proposed design methods and produced SHA-256 core. The proposed SHA-256 operation block results in a 170% increase of throughput and 35% area increase. This area penalty is about 10% for the whole security scheme that we considered for the IPSec and which also includes AES encryption algorithm. This is based on the fact that an IPSec core includes the AES, hash function and the corresponding control logic. Based on previous AES implementations [Hodjat et al. 2004; Granado-Criado et al. 2010] it is derived that their area sizes are similar to that of the of the SHA-256 core. Thus, assuming a 10% area overhead for the control logic the area penalty is about 10% for the whole security scheme. Since recent implementations of AES have much higher throughput and operating frequencies, this means that the proposed implementation achieves a great increase of throughput for the whole security scheme with a minor area penalty.

To the best of authors' knowledge an HMAC implementation that incorporates the SHA-256 hash function unit does not exist in the literature. Thus, we provide in Table II the implementation results (Post P&R) of the proposed HMAC architecture without comparisons, in a wide variety of FPGAs and speed grades.

As it is shown in Table I, the achieved throughput after place and route in Virtex 6 technology is 10.8 Gbps.

10. CONCLUSIONS

A novel hardware design and implementation of SHA-256 hash function and of corresponding HMAC mechanism for use in high-throughput demanding applications like IPSec was presented. The proposed design presents significant improvement both in throughput and throughput/area cost factor and outperforms when compared to all previously proposed, either by academia or industry, designs and implementations. Certain modifications have been applied on the optimization design methodology that the authors had presented in Michail et al. [2009]. The modified optimization procedure led to the optimized SHA-256 hash core.

The proposed implementation has a throughput of 11Gbps for SHA-256, which is the best performing FPGA implementation that has been reported. This also results in an analogous performance for the whole HMAC mechanism and the corresponding security scheme. Significant design effort was paid to keep area small as well. The experimental results showed that a negligible area penalty was introduced for achieving such a high throughput.

REFERENCES

CAST INC. SHA-256 Core. Commercia IP datasheet. http://www.cast-inc.com/cores.

CERF, V. 2010. Vint Cerf pushes for NZ IPv6 transition., *Computer World* Portal. Press Room. http://computerworld.co.nz/news.nsf/news/vint-cerf-pushes-for-nz-ipv6-transition.

CHAVES, R., KUZMANOV, G. K., SOUSA, L. A., AND VASSILIADIS, S. 2006. Improving SHA-2 Hardware Implementations. In *Proceedings of the Workshop on Cryptographic Hardware and Embedded Systems (CHES '06)*. 298–310.

CHAVES, R., KUZMANOV, G. K., SOUSA, L. A., AND VASSILIADIS, S. 2008. Cost-efficient SHA hardware accelerators. *IEEE Trans. VLSI Syst. 16*, 8, 999–1008.

DOBBERTIN, H. 1996. The status of MD5 after a recent attack. *RSALabs' CryptoBytes. 2*, 2.

DOMINIKUS, S. 2002. A hardware implementation of MD4-family hash algorithms. In *Proceedings of the IEEE International Conference on Electronics Circuits and Systems (ICECS·02)*. 1143–1146.

DORASWAMY, N. AND HARKINS, D. 2003. *IPSec—The New Security Standard for the Internet, Intranets and Virtual Private Networks*. 2nd Ed. Prentice-Hall PTR Publications.

FRIEDL, S. 2003. An illustrated guide to IPSec. http://www.unixwiz.netltechtips/iguide-ipsec.html.

GLABB, R., IMBERT, L., JULLIEN, G., TISSERAND, A., AND VEYRAT-CHARVILLON, N. 2007. Multi-mode operator for SHA-2 hash functions. *J. Syst. Archit. 53*, 2–3, 127–138.

GRANADO-CRIADO, J. M., VEGA-RODRIGUEZ, M. A., SANCHEZ-PEREZ, J. M., AND GOMEZ-PULIDO, J. A. 2010. A new methodology to implement the AES algorithm using partial and dynamic reconfiguration. *Integration, VLSI J. 43*, 72–80.

HELION TECHNOLOGY LTD. Data security products. Commercial IP datasheet. http://www.heliontech.com/auth.htm.

HODJAT, A. AND VERBAUWHEDE, L. 2004. A 21.54 Gbits/s fully pipelined AES processor on FPGA. In *Proceedings of the 12th Annual IEEE Symposium on Field-Programmable Custom Computing Machines*. IEEE Computer Society, Los Alamitos, CA, 308–309.

JOHNSTON, D. AND WALKER, J. 2004. Overview of IEEE 802.16 security. *IEEE Secur. Priv. 2*, 3, 40–48.

KHAN, E., EL-KHARASHI, M. W., GEBALI, F., AND ABD-EL-BARR, M. 2005. A reconfigurable hardware unit for the HMAC algorithm. In *Proceedings of the 3rd International Conference on Information and Communication Technology*. 861–874.

KIM, M., KIM, Y., RYOU, J., AND JUN, S. 2007. Efficient implementation of the keyed-hash message authentication code based on SHA-1 algorithm for mobile trusted computing. In *Proceedings of the 4th International Conference on Autonomic and Trusted Computing (ATC'07)*. 410–419.

KIM, T., JAO, W. I., AND TJANG, S. 1998. Arithmetic optimization using carry-save-adders. In *Proceedings of the 35th Annual Design Automation Conference (DAC'98)*. ACM, New York, NY, 433–438.

KIM, Y., RYOU, J., AND JUN, S. 2009. Efficient hardware architecture of SHA-256 algorithm for trusted mobile computing. In *Proceedings of the 4th International Conference on Information Security and Cryptology*. Revised Selected Papers, M. Yung, P. Liu, and D. Lin, Eds., Lecture Notes In Computer Science, vol. 5437, Springer, 240–252.

Loeb, L. 1998. *Secure Electronic Transactions: Introduction and Technical Reference*. Artech House Publishers. Norwood, MA.

McEvoy, R. P., Crowe, F. M., Murphy, C. C., and William, P. 2006. Optimisation of the SHA-2 family of hash functions on FPGAs. In *Proceedings of the IEEE Annual Symposium on VLSI (ISVLSI '06)*. 317–322

Michail, H. 2010. Cryptography in the Dawn of IPv6. *IEEE GOLDRush Newsl.* 17.

Michail, H., Kakarountas, A. P., Milidonis, A., and Goutis, C. E. 2009. A top-down design methodology for ultra high-performance hashing cores. IEEE Trans. Depend. Secure Comput. 6, *4*, 255–268.

Michail, H., Milidonis, A., Kakarountas, A. P., and Goutis, C. E. 2005. Novel high throughput implementation of SHA-256 hash function through pre-computation technique. In *Proceedings of the IEEE International Conference on Electronics, Circuits and Systems (ICECS '05)*. 240–244.

NIST: SP800-77. 2005. *Guide to IPSec VPN's*. National Institute of Standards and Technology Publications.

NIST-FIPS. 2002a. Digital signature standard federal information processing standard. (FIPS) Publication 186-1, NIST, US Department of Commerce.

NIST-FIPS. 2002b. The keyed-hash message authentication code (HMAC) federal information processing standard. (FIPS) Publication 198, NIST, US Department of Commerce.

NIST-FIPS. 2008. Secure hash standard. (FIPS) Publication 180-3. NIST, US Department of Commerce.

NIST-SHA3. 2011. Cryptographic hash algorithm competition. http://csrc.nist.gov/groups/ST/hash/sha3/index.html.

Perset, K. 2008. Internet address space: Economic considerations in the management of ipv4 and in the deployment of IPv6. Ministerial background report by organization for economic co-operation and development. *GECD Ministerial Meeting on the Future of the Internet Economy*.

Pouffary, Y. 2000. IPv6 networking for the 21st century. In *Proceedings of IPv6 Advantages*.

RFC1321. 1992. The MD5 message digest algorithm. IETF Publications. http://tools.ietf.org/html/rfc1321

RFC2104. 1997. HMAC: Keyed-hashing for message authentication. IETF Publications. http://tools.ietf.org/html/rfc2104.

RFC4303. 2005. IP Encapsulating security payload (ESP). IETF Publications. http://tools.ietf.org/html/rfc4303

Rogawski, M., Xin, X., Homsirikamol, E., Hwang, D., and Gaj, K. 2009. Implementing SHA-l and SHA-2 standards on the eve of SHA-3 competition. In *Proceedings of the 7th International Workshop on Cryptographic Architectures Embedded in Reconfigurable Devices (CryptArchi'09).*

Sklavos, N. and Koufopavlou, O. 2005. Implementation of the SHA-2 hash family standard using FPGAs. *J. Supercomput. 31*, 227–248.

Softjin Electronic Design. SHA 224/256/384/512 Core. Commercial IP datasheet. http://www.heliontech.com/auth.htm.

SSL. 1998. Introducton to SSL. http://docs.sun.com/source/816-6156-10/contents.htm.

Ting, K. K., Yuen, S. C. L., Lee, K.-H., and Leong, P. H. W. 2002. An FPGA based SHA-256 processor. In *Proceedings of the 12th International Conference on Field Programmable Logic and Applications.* M. Glesner, P. Zipf, and M.Renovell, Eds., Lecture Notes in Computer Science, vol. 2438, Springer, 577–585.

Wang X., Yin, Y. L., and Yu, H. 2005. Finding collisions in the full SHA1. In *Proceedings of the 25th Annual International Cryptology Conference.* Lecture Notes in Computer Science, vol. 3621, Springer, 17–36.

Zeghid, M., Bouallegue, B., Baganne, A., Machhout, M., and Tourki, R. 2007. A reconfigurable implementation of the new secure hash algorithm. In *Proceedings of the 2nd International Conference on Availability, Reliability and Security*. IEEE Computer Society, Los Alamitos, CA, 281–285.

Zeghid, M., Bouallegue, B., Baganne, A., Machhout, M., and Tourki, R. 2008. Architectural design features of a programmable high throughput reconfigurable SHA-2 Processor. *J. Inf. Assur. Secur. 2*, 147–158.

Received August 2010; revised June 2011; accepted July 2011